Int. J. Electrochem. Sci., 8 **(2013)** 5560 - 5574

International Journal of
ELECTROCHEMICAL
SCIENCE
www.electrochemsci.org

Electrocatalytic Oxidation of 1-Butyl-3-Methylimidazolium Chloride: Effect of the Electrode Material

Ewa M. Siedlecka[1,*], *Aleksandra Fabiańska*[1], *Stefan Stolte*[2], *Anne Nienstedt*[2], *Tadeusz Ossowski*[1], *Piotr Stepnowski*[1], *Jorg Thöming*[2]

[1]Faculty of Chemistry, University of Gdańsk, ul. Sobieskiego 18, 80-952 Gdańsk, Poland
[2]UFT-Centre of Environmental Research and Sustainable Technology, University of Bremen, Leabener Straße UFT, D-28359 Bremen, Germany
[*]E-mail: ewas@chem.univ.gda.pl

Received: 1 February 2013 / *Accepted:* 28 February 2013 / *Published:* 1 April 2013

Aqueous process diluted solutions containing ionic liquids (ILs) are a challenge for water treatment as many ionic liquids are not biodegradable and hazardous for the environment. As an advanced oxidation process electrochemical depletion of the 1-butyl-3-methylimidazolium chloride (IM14Cl) dissolved in water was studied using dimensionally stable anodes (IrPt, IrO_2, PbO_2) and boron-doped diamond (BDD). Cyclic voltammetry demonstrated that electrochemical oxidation of the $IM14^+$ mainly occurred indirectly via •OH and by other chemical entities such as active chlorine species. Next, ionic liquid oxidation was carried out galvanostatically in the potential region of water discharge. The conventional electrodes (IrPt, IrO_2) were ineffective for the removal of IM14Cl. As the IrO_2 anode surface was deactivated by organic intermediates generated in this process, IM14Cl degradation was not complete and COD removal was very low (19%). Effective electrochemical oxidation was achieved at "non-active" electrodes like PbO_2 and BDD. At the lowest used current density COD removal was 60% and 84% for PbO_2 and BDD respectively. To better understanding the mechanism of IL electrooxidation by-products were identified by GC-MS technique. The results suggested that the electrolysis at "active" and "non-active" electrode materials led to the different distribution of products, due to different mechanism of IL degradation.

Keywords: Advanced oxidation process; electrochemical oxidation; dimensionally stable anodes; ionic liquids; wastewater treatment

1. INTRODUCTION

Ionic liquids (ILs) are a versatile class of low melting point organic salts that typically have low vapour pressure at room temperature. They are increasingly being used as solvents, catalysts, in lithium-ion batteries [1] in dye-sensitized solar cells [2] or as lubricants [3] and paint additives [4].

With this growing number of industrial applications they will sooner or later turn up in industrial wastewaters. Moreover, some applications need chemically stable, often non-biodegradable ILs, which after use ought to be regenerated or recovered, but even so will eventually appear in wastes. Most imidazolium-based ILs are not readily biodegradable and have been found to have adverse effects on bacteria, algae, earthworms and zebrafish [5-11]. Therefore, the release of these chemicals into the environment is going to be a problem, so removal options have to be developed.

Traditional biological, physical and chemical treatment methods are often ineffective for non-biodegradable and/or toxic organic compounds; discharged into surface waters, effluents containing these pollutants can give rise to several environmental problems. Electrooxidation appears to be a most promising technology for the treatment of water and wastewater containing small amounts of organic pollutants: its distinct advantages include environmental compatibility, versatility, energy efficiency, safety, amenability to automation and cost effectiveness. Electrochemical oxidation at anodes made of graphite, Pt, TiO_2, IrO_2, PbO_2, several Ti-based alloys and, more recently at boron-doped diamond (BDD) electrodes, has been employed for the decontamination of effluents containing various organics like phenols [12] pharmaceuticals [13] alcohols, carboxylic acids [14], anionic surfactants [15] and pesticides [16]. These investigations have shown that the effectiveness of electrochemical treatment depends very closely on the electrode material. The possible mechanisms of electrochemical oxidation are essentially based on oxygen-transfer stages in which electrosorbed hydroxyl radicals should play the decisive part. Therefore, the dimensionally stable anodes (DSA) used in industrial electrochemistry, which are characterized by a low oxygen overvoltage (Pt, IrO_2), perform much worse than electrodes with a high overvoltage of oxygen evolution (PbO_2, BDD). However, IrO_2 electrode can be successful used to antibiotic or lignine decay [17, 18]. The electrodes with a high overvoltage of oxygen evolution also have their shortcomings: for example, BDD electrodes are much more expensive than IrO_2 or PbO_2 electrodes, an important disadvantage in industrial applications. he use of a lead dioxide electrode, with its high electrical conductivity, high oxygen overvoltage and low cost compared with BDD, can achieve a high efficiency and lower the operating cost, but its main drawback is the leaching of toxic lead ions to solution.

According to literature reports, IL degradation has been studied in photocatalytic processes [19] Fenton and Fenton-like reactions [20-21] and electrochemical processes at bipolar BDD [8] or at BDD electrodes [22]. The mechanism of imidazolium IL degradation at different kinds of electrodes has not yet been elucidated, and electro-oxidation intermediates haven't been identified and compared. In our investigations, the ionic liquid decomposition at anodes with low and high overvoltage of oxygen evolution was compared.

The aim of the present work was to increase our understanding of the mechanism involved in the electrooxidation of imidazolium-based IL in view of electrode material. The research was carried out at Pt/Ir, IrO_2, PbO_2 and Si/BDD electrodes, all of which are used in industrial applications. The intermediates of ILs electrooxidation at different anodes were identified and compared for the first time. Their identification of intermediates is very important from both the application and environmental poin of view.

2. EXPERIMENTAL

2.1. Chemicals

1-Butyl-3-methyl-imidazolium chloride (IM14Cl), H_3PO_4 and KH_2PO_4 were obtained from Merck KGaA (Germany), Na_2SO_4 was purchased from Gruessing GmbH Analytika, (Germany), H_2SO_4 from Fisher Scientific GmbH (Germany), acetonitrile (HPLC grade) from Sigma-Aldrich Chemie GmbH (Germany), and methanol from VWR International GmbH (Darmstadt, Germany)

2.2. Electrochemical measurements

Cyclic voltammetry (CV) was carried out in a typical three-electrode system on a potentiostat/galvanostat (PGSTAT-30 Autolab) connected to a computer as an electrochemical workstation. IrPt, IrO_2 and PbO_2 electrodes of surface area 1.7 cm^2 (De Nora Germany) and Si/BDD electrodes of surface area 1 cm^2 (Adamant Technologies) were used as the working electrode; Ag/AgCl was the reference electrode and a Pt wire was the counter electrode. The concentrations of IM14Cl in 87 mM Na_2SO_4 supporting solution were 0.1, 0.5 and 1 mM. All measurements were performed at room temperature (20 ±2°C) in 5 or 20 ml reactors. CV was repeated until reproducible signals were obtained. The CV curves were recorded up to the decomposition potential of water and/or the supporting electrolyte.

2.3. Electrochemical oxidation of IM14Cl

Electrochemical degradation was performed with 0.21 mM aqueous solution of IM14Cl with 87 mM Na_2SO_4 added as support electrolyte. The electrochemical decomposition experiments were carried out in an undivided electrolytic cell equipped with anodes made from different materials: IrPt, IrO_2, PbO_2 (De Nora Germany) and Si/BDD (Adamant Technologies SA). Stainless steel no. 1.4401 (X5CrNiMo17-12-2) was used as cathode and Ag/AgCl as reference electrode. The anode elements (IrPt, IrO_2, PbO_2) consisted of expanded metal with an active surface area of 125 cm^2. The cathode element was a flat piece of steel (surface area = 131 cm^2). In the experiments carried out with BDD the active surface area of both the anode and the stainless steel cathode was 10 cm^2. The distance between the electrodes in all cases was 1 cm. The experiments were performed at constant current densities: 8, 16 and 24 mA cm^{-2}. The temperature of the solution in the electrolytic cell was kept constant by a UB 30 thermostat (Lauda Dr. R. Wobser GmbH & Co. KG, Königshofen, Germany) and a magnetic stirrer. A power supply unit (Statron Gerätetechnik GmbH, Germany) was used to adjust the total current manually.

To follow the progress of IM14Cl degradation during 3h of electrolysis, samples were taken at appropriate intervals of time and IL concentrations measured by HPLC-UV analysis. Hence the decrease in parent compound concentration and the appearance and disappearance of intermediates absorbing at 212 nm could be detected.

The energy consumption per volume of treated effluent was estimated and expressed in kilowatt hours per cubic metre. The average cell voltage during the electrolysis (cell voltage is reasonably constant with just some minor oscillations, for this reason, the average cell voltage is calculated), is taken for calculating the energy consumption, as follows [23]:

$$\text{Energy consumption} = \left(\frac{V \times A \times t}{1{,}000 \times V_s}\right)$$

where t is the time of electrolysis (hours); V and A are the average cell voltage (volts) and the electrolysis current (amperes), respectively; and V_s is the sample volume (cubic metre).

2.4. Analytical methods

AOXs and CODs were measured after 3h of electrolysis by using cuvette tests LCK 391 and 314 respectively and a Cadas 200 spectrophotometer (Hach-Lange GmbH). The pH was measured with a pH-meter (WTW). The progress of IL elimination and the identification of electrolysis products were quantified using HPLC and GC-MS respectively.

According to [24] N, N-dimethyl-p-nitrosoaniline (RNO) was used to determine the number of •OH radicals. Electrolysis was then applied in a 100 ml phosphate buffer (pH=7.1) solution containing 0.03 mM RNO. The bleaching of the yellow colour was measured at λ=440nm and the concentration of OH radicals during electro-oxidation was calculated using Eq.

$[OH] = 1-[RNO]/[RNO_0]$,

where [OH] is the hydroxyl radical concentration, and $[RNO_0]$ and [RNO] are the respective concentrations of N, N-dimethyl-p-nitrosoaniline initially and after time *t*.

2.5. HPLC

For determining the electrochemical degradation, a HPLC VWR Hitachi system ("LaChrome Elite") was used, containing an L-2130 HTA-pump, L-2130 degasser, L-2200 autosampler, L-2350 column oven, L-2450 diode array-detector and EZ Chrome Elite software. A cation exchanger with a guard column (CC 125/4 Nucleosil 100-5SA; Macherey-Nagel, Düren, Germany) was employed. The mobile phase consisted of 55 or 53 % acetonitrile (HPLC grade) and 45 or 43 % aq. KH_2PO_4 (25 mM) and H_3PO_4 (3.2 mM). The system was operated at a flow rate of 1 or 0.75 mL min^{-1} and 10 µL portions of the samples were injected. A detection wavelength of 212 nm was used for IL quantification. The limit of HPLC-UV detection was ca 3 µM.

2.6. GC-MS

For the identification of the intermediates GC-MS system was used. Mass spectra (70 eV) were recorded on a SSQ-710 mass spectrometer (Finnigan). The ion source was maintained at 220°C. The samples were introduced through a Hewlett-Packard 5890 gas chromatograph equipped with a capillary column. The carrier gas was helium. For analysis, the injector and transfer line temperatures

were 310°C. A RTX-5 fused silica column (30m x 0.25mm i.d., film thickness 0.25 μm) was used. The GC was programmed from 50°C to 310°C at the rate of 4°C/min.

3. RESULTS AND DISCUSSION

3.1. Cyclic voltammetry

Cyclic voltammetry has been carried out to obtain information about the electroactivity of IM14Cl at IrPt, IrO_2, PbO_2 and BDD electrodes. Fig. 1 shows the cyclic voltammetry curves of IM14Cl at PbO_2, BDD and IrO_2 anodes, which were obtained in the absence (blank solution) and presence of dissolved ionic liquid at concentrations 0.5 mM and 1.0 mM .

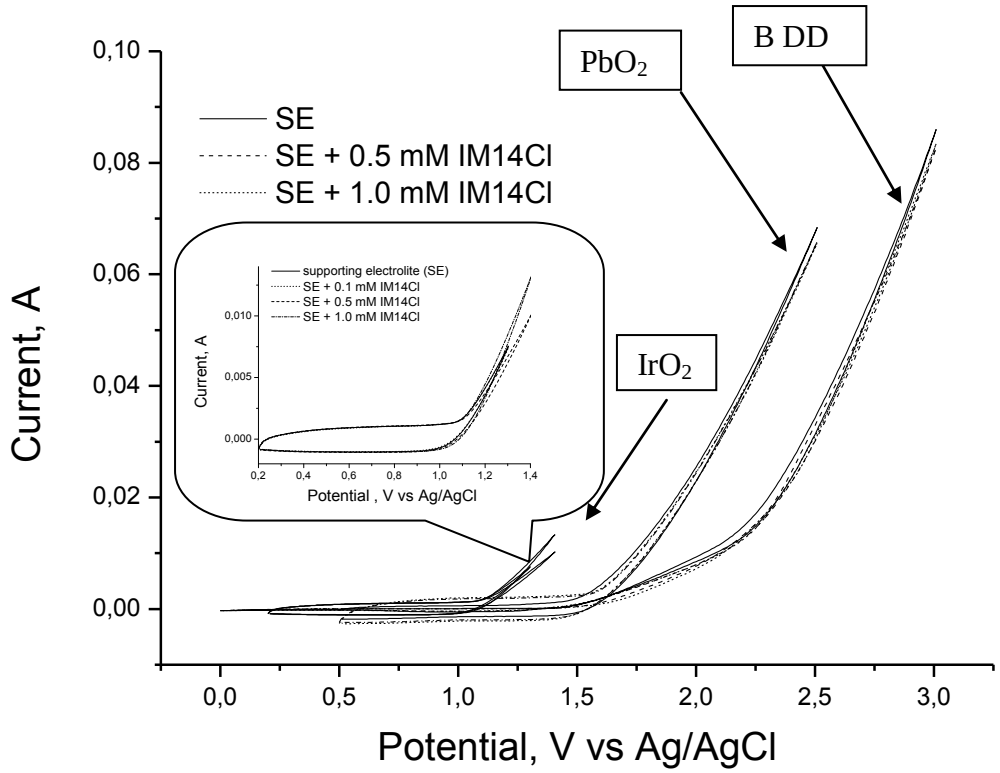

Figure 1. CV curves for the IrO_2 a), BDD b) and PbO_2 c) in the presence of the water/supporting electrolyte 87mM Na_2SO_4 and IM14Cl in solution at different concentrations. Scan rate 100mV/s.

As it can be seen at Fig. 1, the studied electrodes were characterized by different potential of oxygen evolution. The electrochemical activity was analysed at two potential windows: i) one where no oxygen evolution takes place, so organic matter is oxidized directly, based on electron transfer between the electrode surface and the adsorbed substrate, and ii) another where high current densities are employed to generate oxygen entities for the mediated oxidation of organic pollutants. Compared

with the curve obtained in the blank solution there was no additional anodic current peak during the positive sweeps in the first range analysed, indicating that no significant direct oxidation of the ionic liquid had occurred. Similar behaviour was observed for all anode materials.

In the oxygen evolution regime an increase in the onset potential of oxygen evolution as an effect of increasing of concentration of IM14Cl was observed only for IrO_2 anode The increase in IM14Cl concentration from 0,1mM to 1mM caused the shift of the anodic current to lower potentials. At the BDD and PbO_2 anodes, addition of IM14Cl to the solution resulted in non-significant changes in the anodic current potential.

As expected, the results clearly indicated that $IM14^+$ could only be indirectly oxidized on these anodes at the oxygen evolution potential. Of the investigated anodes the IrO_2 anode has the best adsorption properties [25]. Therefore, IrO_2 may adsorb organic compounds (probably by-products), resulting in its partial passivation, after which the current shifts to a higher potential range. On the other hand, a further increase in IM14Cl concentration to 0.5 mM gives rise to an anodic current. Such behaviour is known from the literature [26] it can be attributed to the oxidation of the Cl^- anion of IL to Cl_2. The increase of Cl^- concentration to 0.5 mM as a result of the increase in IL concentration was enough to observe this process.

BDD is characterized by weaker adsorption properties and much higher overpotential oxygen evolution than PbO_2 and IrO_2 electrodes. However at this anode the oxidation of IM14Cl in direct way was also not observed. CV experiments clearly show that oxidation of IM14Cl depends on the discharge of water at all the tested electrodes. As expected, the $IM14^+$ cation can be oxidized indirectly by strong oxidants such as hydroxyl radicals (E^0 = 2,8 V vs. NHE), or by other oxidants (active chlorine species: Cl_2 E^0 = 1.44 V, HClO E^0 = 1.579V, ClO_2 E^0 = 1.59 V, $HClO_2$ E^0 = 1.65 V or ozone E^0 = 2.07V) generated in at the anode surface.

3.2. Electrocatalytic oxidation experiments

The study reports the electrochemical oxidation under galvanostatic conditions of an aqueous dilute solution of ionic liquid at different anode materials: PbO_2, BDD, IrO_2 and IrPt. To investigate the effect of different operating factors on the rate of electrochemical degradation, a series of experiments was carried out at current densities 8, 16 and 24 mAL^{-1} and different IM14Cl concentrations (37 and 72 mgL^{-1}). The current densities were selected in order to operate at the water/supported electrolyte discharging regime where the oxidation reactions take place.

3.2.1. Kinetic study of IM14Cl degradation

In kinetic analysis of the results obtained for IM14Cl (37 mg/L) at BDD, PbO_2 and IrPt we found that only pseudo-first-order reaction rate equations let to satisfying correlations. The pseudo-first-order rate constants *k* obtained for IL electro-oxidation at BDD, PbO_2 and IrPt are presented in Table 1. For comparing the electrical charge needed for IL degradation, the changes in IL concentration with electrical charge (Q) are depicted in Fig.2 and Fig. 3.

With decreasing current density the corresponding *k* progressively drops for all electrode materials (Table 1). At all the investigated current densities for BDD and PbO_2 IL was almost totally removed by an electrical charge lower than 9 AhL^{-1} (Fig. 2). At the IrPt electrode IM14Cl oxidation was slow and the electrical charge consumed for total IL removal was 25.4 AhL^{-1} (Table 2). In addition, the effect of current density on the value of *k* is far less than with the other electrodes (Table 1).

Table 1. The pseudo-first-order kinetic rate coefficient (*k)* and energy consumption at different current density for different anode materials.

Electrode material	Current density ($mA\ cm^{-2}$)	Concentration of IM14Cl (mgL^{-1})	k (min^{-1})	Correlation coefficient (R^2)	Energy consumption* kWh/m^3
BDD	8	36	0.010	0.997	13.5
	16	36	0.018	0.996	17.1
	24	36	0.020	0.991	29.0
PbO_2	8	36	0.007	0.994	45.9
	16	36	0.014	0.998	62.0
Ir/Pt	8	36	0.002	0.989	92.3
	16	36	0.003	0.983	163.8

- total IL removal

In contrast to the previously mentioned anodes, two stages in the IM14Cl degradation reaction were observed at IrO_2 (Fig. 2). The first stage of electrodegradation followed the pseudo-first-order rate, but in the next stage the reaction was almost completely inhibited. Consequently, only 62% of the initial concentration of IM14Cl was removed at 8 $mA\ cm^{-2}$.

BDD

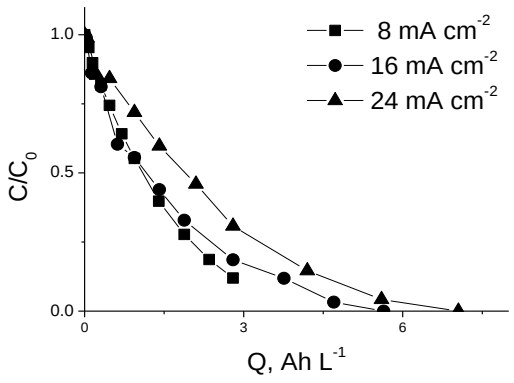

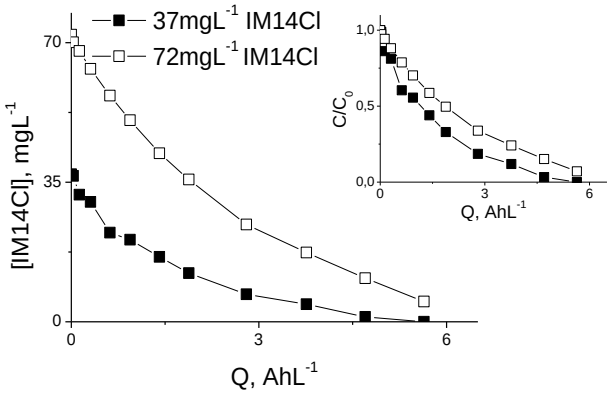

PbO_2

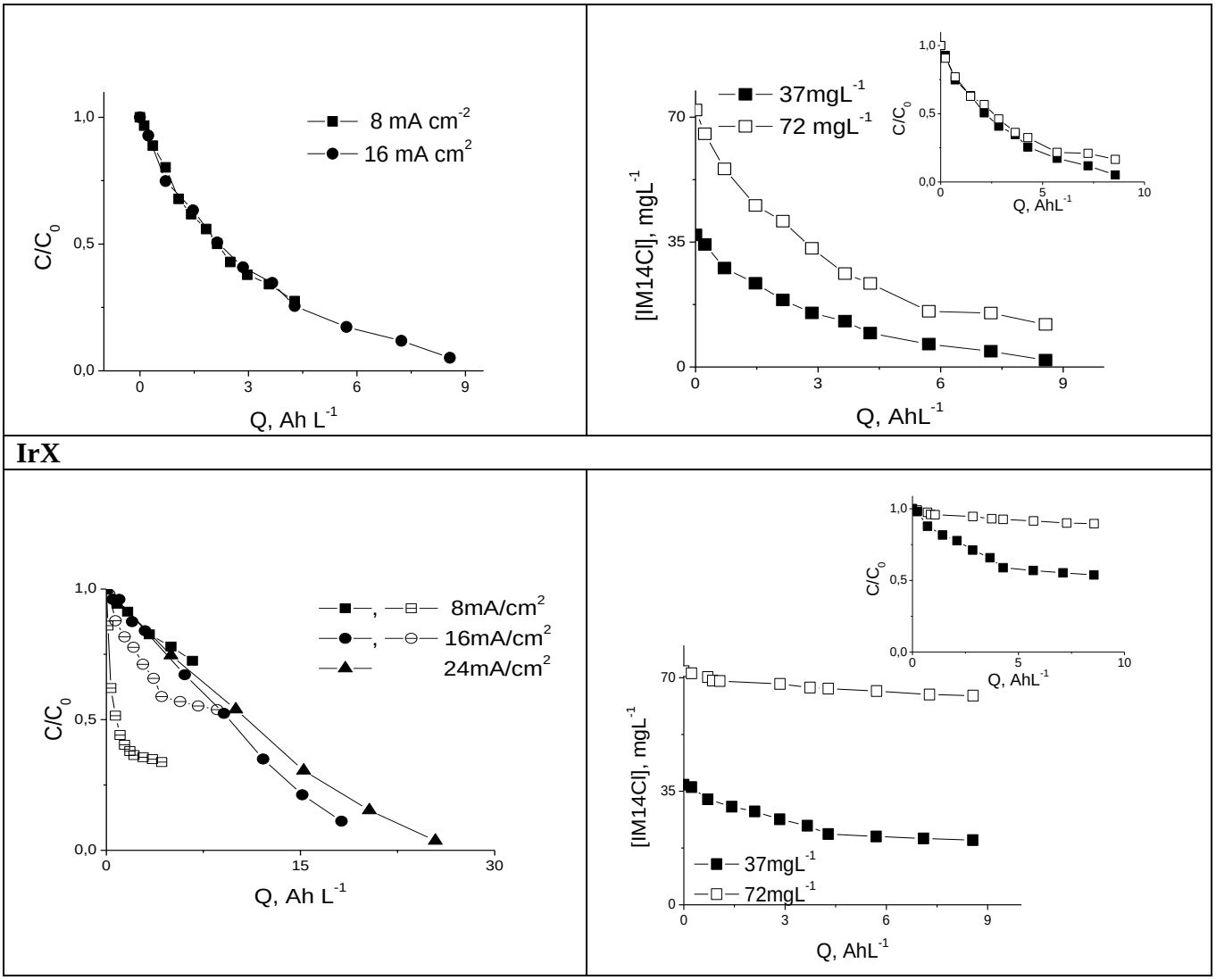

Figure 2. Variation of IM14Cl concentration during electrolysis at four different anodes in relation with current density and initial concentration of ionic liquid in 87mM Na_2SO_4.

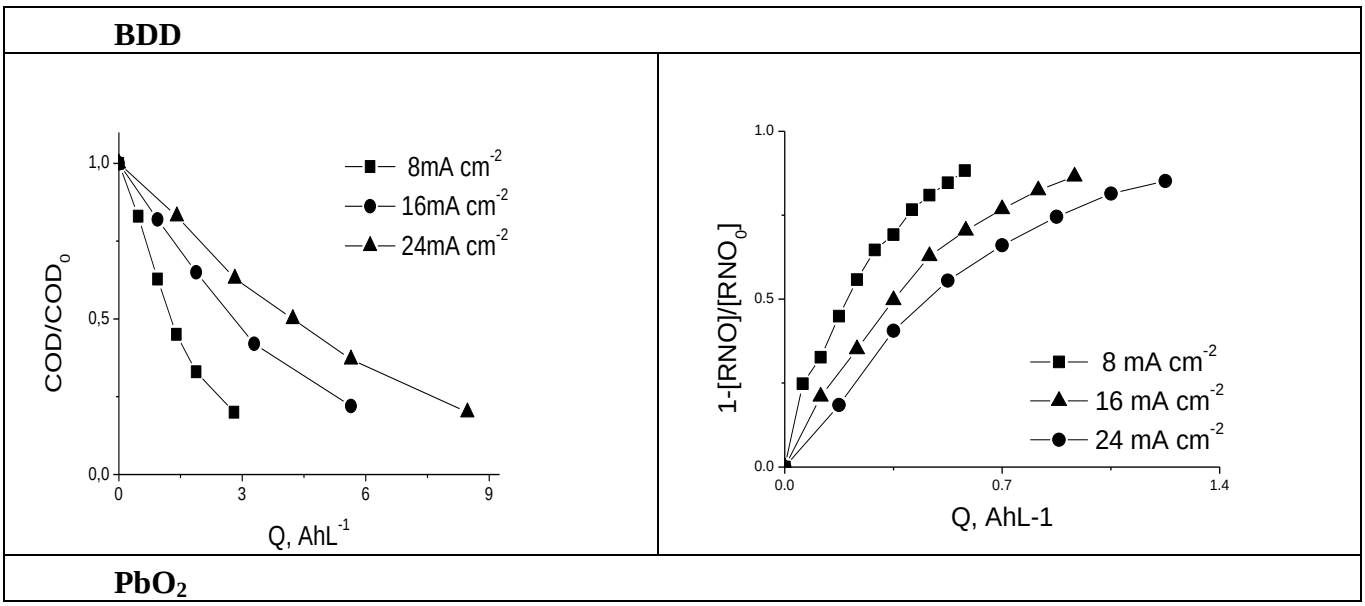

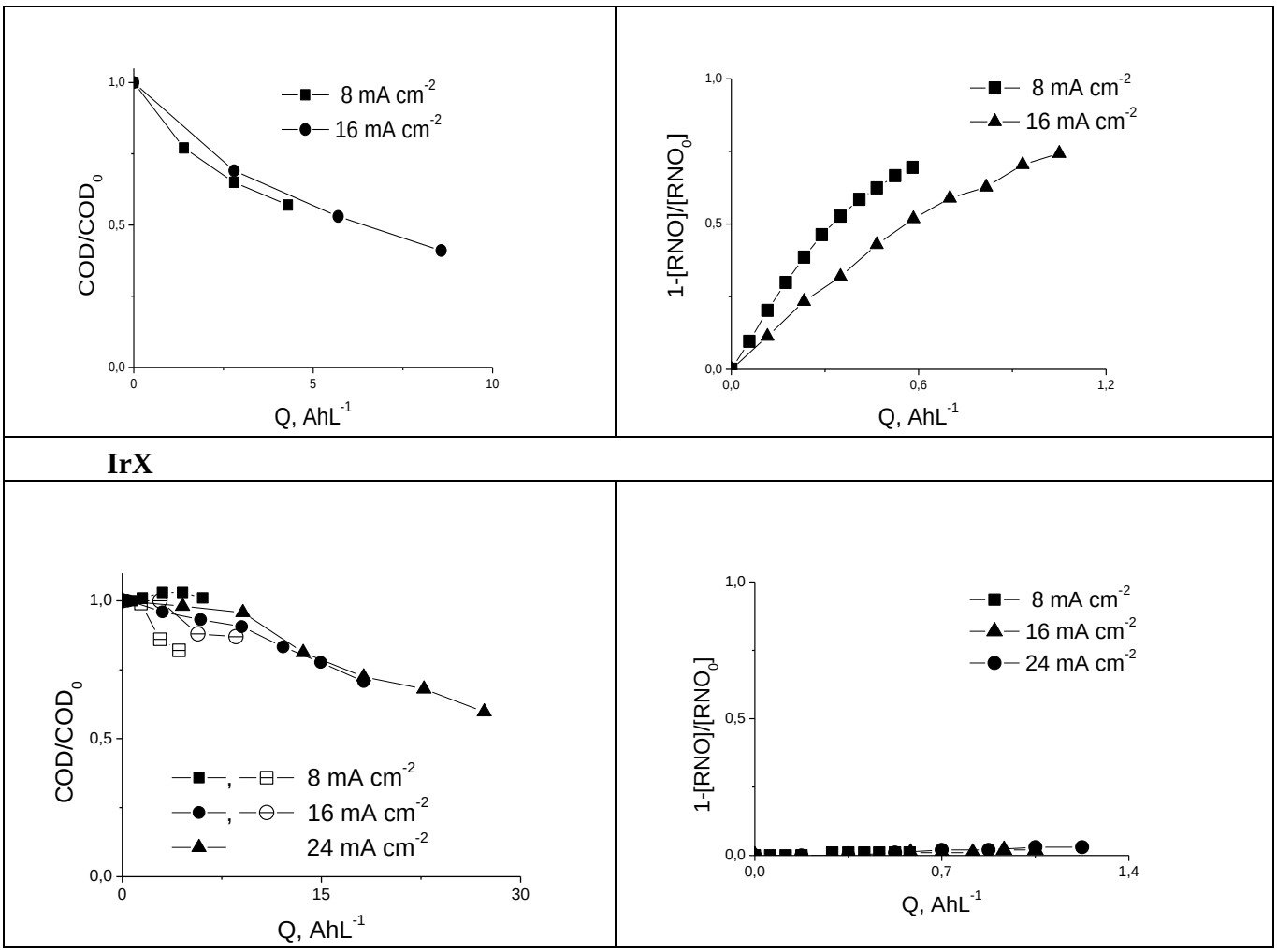

Figure 3. Variation of COD during 37mg L^{-1} IL degradation in 87mM Na_2SO_4 and •OH radicals concentration during electrolysis in buffer phosphate (pH=7.1) at four different anodes in relation with current density. ■, ● – Ir/Pt, □, ○ – IrO_2.

Next, the reaction rate between IL and oxidant species generated at different anode materials was studied for two IL concentrations 37 mg/L and 72 mg/L at a fixed current density 16 mA cm^{-2} (Tables 1).

An increase in IL concentration caused a decrease in the value of *k* for BDD and IrO_2 anode. In contrast to this it was similar for PbO_2 electrode.

Obtained results (Table 1 and Fig. 2) indicated that at "non-active" electrodes (PbO_2 and BDD) the lowest current density was enough for removing 0.21 mM IL from water solution.

An increase of current density from 8 to 24 mA cm^{-2} at BDD anode did not enhance IL oxidation and thus meant to waste electrical charge enhancing side reactions. IL concentration also influenced on the rate and efficiency of electrooxidation at BDD. This can be explained by the fact that a higher initial concentration of IL demands larger amounts of electrogenerated oxidants like •OH radicals for rapid degradation. This also means that the reaction between •OH radicals and IL was not in the pseudo-first kinetic order in system. The decrease of *k* from 0.018 to 0.012 confirmed that at

BDD IL reacted with a practically constant concentration of oxidants, like the •OH radicals generated at this anode surface, but their concentration is not enough high that reaction dependent only on IL concentration However, there were differences in the degradation mechanisms of IL at PbO_2 anode, where the increase of concentration not have influence on the k. On the other hand, the increase in IL concentration lowered the oxidation efficiency more for PbO_2 than for BDD electrode (data not shown). This indicated that some by-products generated during electrolysis were harder to oxidize at the PbO_2 electrode than the BDD.

3.2.2. Oxidation of organic matter

As is evident from the results in Fig. 3, the increase of current density was responsible for decrease of charge specific oxidation efficiency (expressed as COD/COD_0) at the BDD and PbO_2 electrodes. This is due to the fact that the higher current densities were clearly above the limiting current density for oxygen evolution reaction. Thus the higher the current density especially at BDD, the more charge is spent for oxygen evolution without affecting the anodic provision of oxidant for IL depletion.

IM14Cl oxidation at the IrPt electrode was complete but very slow, and COD removal was only 19 %. This trend could be accounted for by the formation of intermediates, which were poorly oxidizable at this electrode and remained in solution to the end of the experiment.

In contrast to the electrodes described above, the shape of the curve for IrO_2 indicated deactivation at the anode surface. Such behaviour of IM14Cl at the IrO_2 anode suggested that the oxidation reaction might be mediated by active species (•OH radicals strong adsorbed to surface of anode, active chlorine) generated at the anode surface, which "depolarises" the anode preventing oxygen formation. Deactivation of the active centres needed for oxidant generation is due to adsorption of some organic matter.at anode surface.

The shape of the electrochemical oxidation-time profile obtained for IrO_2 was similar in the potential region before oxygen evolution at the BDD anode during the oxidation of aromatic compounds. No electrocatalytic activity was reported for the oxidation of organic compounds, which resulted in BDD surface deactivation [27-29]

As it was shown previously at IrO_2 anode direct oxidation of Cl^- took a part forming active chlorine species, which in turn are very likely to oxidize organic pollutants and elevate the degradation rate for the cost of formation of organochlorine compounds. This was confirmed measuring adsorbed at carbon organochlorine compounds (AOX). After 3 h of electrolysis with 8 mA cm^{-2} at IrO_2 0.49 mg L^{-1} of AOX were found. However the concentration of Cl^- was very low (0,24mM), therefore the active centres with adsorbed •OH radicals could play significant role in cation decomposition.

It is known that BDD is a high-oxygen–overpotential material and is therefore expected to perform quite well in the electrochemical mineralization of organic matter [14] Analysis of the results in Fig. 3 indicates that COD removal at the BDD anode is closely correlated with the number of hydroxyl radicals generated on the anode surface. At higher current densities, the formation of the powerfully oxidizing •OH radical is hampered by the generation of side products such as O_2. The

concentration of •OH radicals is therefore lower, as is the efficiency of organics oxidation. These results indicate that electrochemical oxidation of IM14Cl at a BDD anode is mediated mainly by quasi-free •OH radicals but that reactions with other entities are also possible such as peroxodisulphate expected exceed 2.0V.

A similar decrease in •OH radical concentration with increasing current density was observed at the PbO_2 anode (Fig. 3). But in this case the concentration of •OH radicals was not correlated with COD removal. This implies that the reaction between IM14Cl and •OH radicals is not the only decisive factor in this process.

No significant numbers of quasi-free hydroxyl radicals were found during electro-oxidation at the IrO_2 anode (Fig. 3). At this "active" anode, the increase in oxygen evolution with current density also caused a decrease in oxidation efficiency.

The $IM14^+$ oxidation mechanism at an "active" anode could be degradation mediated by •OH radicals strongly interacting with the anode surface or by the other more selective oxidizers such as active chlorine oxidants

3.3. Comparison of electrode materials

The electro-oxidation efficiency of 37 mgL^{-1} of IM14Cl at a fixed current density of 16 mA cm^{-2} at all the electrodes is compared in Fig. 4.

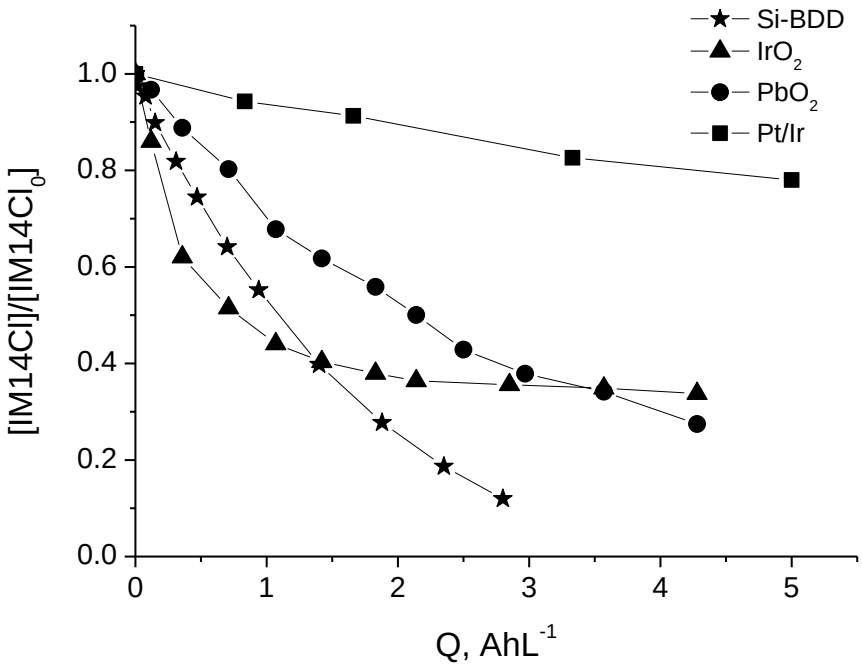

Figure 4. IM14Cl intermediates evolution during electrolysis at four anodes at fixed current density16mA cm^{-2}. Experimental conditions: [IM14Cl] = 72mgL^{-1}, [Na_2SO_4] = 87 mM, initial pH = 6,2.

The IrPt and IrO_2 anodes are much less efficient regarding IM14Cl and COD removal than the BDD and PbO_2 anodes. However in the first stage of reaction the rate of IM14Cl degradation (to $1,4AhL^{-1}$) was the highest for the IrO_2 electrode. It indicated that oxidants generated at IrO_2 (adsorbed •OH radicals, active chlorine oxidants) are effective in IM14Cl decay, but not efficient in decomposition of intermediates. Additionally the adsorption properties of IrO_2 electrode effect at a disadvantage on the oxidation process. It is worth noting that IM14Cl was most efficiently oxidized at the BDD anode. The poorer efficiency at PbO_2 was attributed to the limited number of hydroxyl radicals at the anode surface and also the easier combination with each other to generate oxygen as a side reaction. This is confirmed by an oxygen evolution potential that was lower at PbO_2 than it was at BDD (Fig. 1). In consequence, there are less •OH radicals to react with organic pollutants at the PbO_2 anode. This hypothesis was confirmed by the detection of hydroxyl radicals (Fig. 4c) during the electrolysis of phosphate buffer at PbO_2 and BDD anodes. As expected, the concentration of •OH radicals generated at the PbO_2 anode was less than that at the BDD anode for the same current density. The results suggest that the concentration of quasi free hydroxyl radicals under our experimental conditions is the main factor governing the effective mineralization of the 1-butyl-3-methylimidazolium cation, but not in decomposition of parent compound. At BDD and PbO_2 electrodes oxidants (•OH) reacts with both IM14Cl and intermediates. In contrast, at the "active" electrodes the oxidation process seems to be mainly focused on the parent compound. At IrO_2 electrode high rate of salt decomposition (in the first stage of electrolysis) was likely caused by active chlorine species as well as active centres with strong adsorbed •OH radicals. Production of ozone is also expected, because the anode potential was higher than 1.51 V, which is necessary to its evolution.

The cumulative current efficiency (CE) calculated from COD is presented in Table 1. For the BDD electrode CE ranged from 28 to 62%, depending on the current density and IL concentration. CE was nearly three times less for the PbO_2 anode (14%-20%), which suggests that this organic matter was hardly oxidized at all at the PbO_2 anode. This could have been due to intermediates such as short-chain aliphatic carboxylic acids, which are known to be difficult to oxidize at PbO_2. A similar interpretation of a COD residue during electrolysis at a PbO_2 anode was reached by Sires et al. (2008), who investigated the electrodegradation of phenol compounds [30]. These results indicated that BDD would be the better choice for ionic liquid removal from wastewater.

In order to acquire the information required to elucidate the pathway of IM14Cl oxidation, analyses of GC-MS mixtures for the investigated electrodes were compared. The main intermediates were identified and they are presented in Table 2. Some intermediates with an imidazolium core were found with all anodes. There were 1-methylimidazole (m/z=82), 1-butylimidazole (m/z=124) and imidazole (m/z=68). In contrast to the IrO_2 electrode during electrolysis at BDD and PbO_2, the main intermediates were compounds with oxidized imidazole ring: 1-butyl-3-methylimidazol-2-one (m/z=154) and 1-butyl-3-methylimidazolidine-2,4,5-trion (m/z=184). At PbO_2 anode the intermediate with m/z=130 was also found.

Table 2. Probably intermediates of IM14Cl electrolysis at different anodes

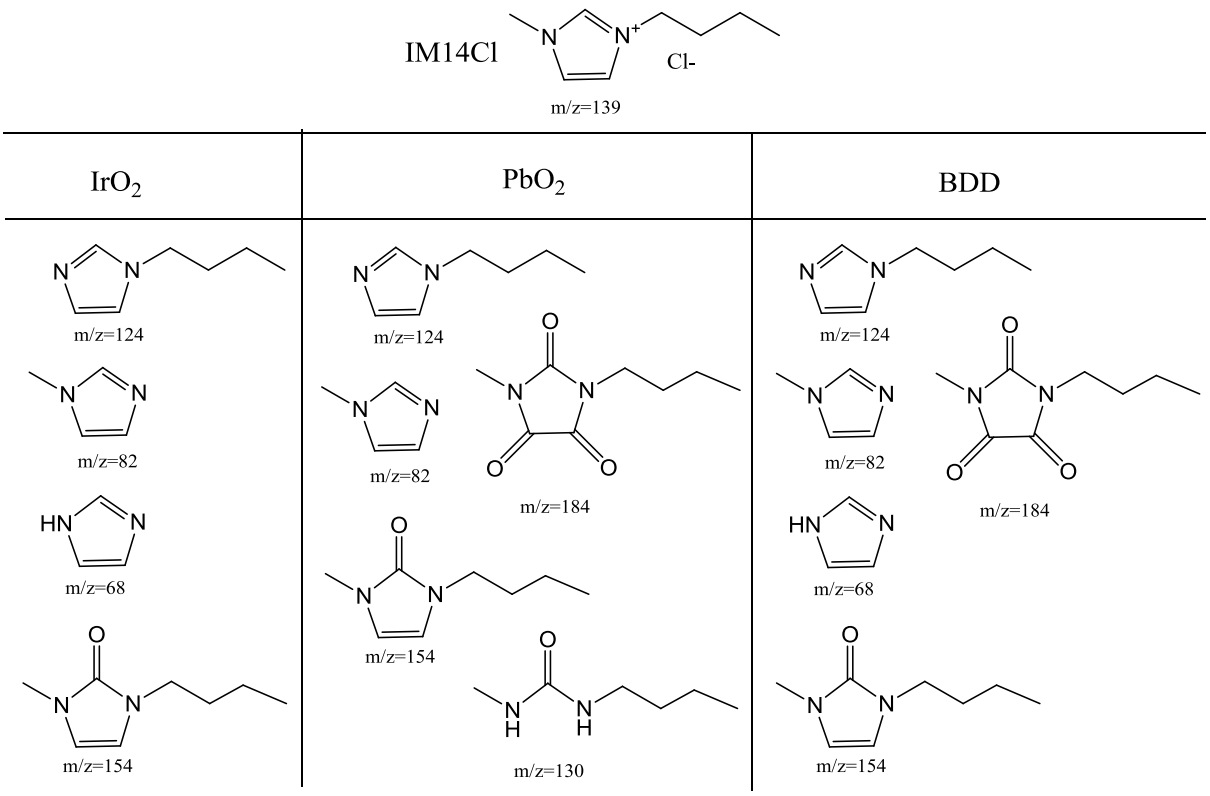

The evolution of intermediates with an imidazolium core at IrO_2 anode and presence of 1-butyl-3-methylimidazol-2-one (m/z=154), 1-butyl-3-methylimidazolidine-2,4,5-trion (m/z=184) at BDD and PbO_2 anodes suggested that the pathway of degradation at "non-active" (BDD, PbO_2) and "active" (IrO_2) electrodes will be different. These results confirm that the electrochemical oxidation of IM14Cl at BDD and PbO_2 is due mainly to •OH radicals, which are the strong and non-specific oxidants, attacking aromatic and aliphatic parts of the IM14Cl molecule. A similar pathway of imidazolium IL degradation was observed during oxidation by AOP processes [18, 31] where the •OH radical is the primarily responsible factor for organic pollutants degradation. At IrO_2 anode the decomposition of imidazolium salt went mainly by cleavage of side chains. This way was also observed at "non-active" electrodes.

4. CONCLUSION

The electrochemical oxidation of 1-butyl-3-methylimidazolium chloride in dilute aqueous solution was investigated at four types of anode materials: IrPt, IrO_2, PbO_2 and BDD. The oxidation of the $IM14^+$ cation at all of them is in indirect way. At the IrO_2 electrode the anion of IM14Cl was oxidized to chlorine species and cation, was decomposed by strong adsorbed •OH radicals and active chlorine species. After 3h of electrolysis the intermediates with the side chains cleavage were found by GC-MS. The main problem observed at this anode was the deactivation of the anode surface by organic matter. At the BDD anode the •OH radical concentration is closely correlated with COD

removal, which suggests that they are main oxidants in IM14Cl degradation at this anode. Also at PbO_2 hydroxyl radicals were the main oxidants of IL but there were also other factors limiting this process. In contrast to "non-active" electrodes, oxidation at "active" electrodes not removes aromaticity in IL, so the biodegradability of organic matters after the electrochemical treatment likely not increased significant. Additionally the presence of chloroorganics could increase the effluent toxicity. At the BDD electrode the effectively mineralizing organic matter was found. However, intermediates obtained by side chains cleavage leading to the generation compounds with imidazolium ring were also observed.

Therefore, the rate of IM14Cl oxidation as well as the current efficiency were higher at the BDD than at the PbO_2 anode, so BDD seems to be the most promising electrode for the elimination of ionic liquids from diluted solution of water. In any case, for all types of electrodes, biodegradability tests and toxicity tests of electrochemically treated solutions should be carried out to allow to assess the environmental friendliness of the concept.

References

1. J. D. Holbrey, N.V. Plechkova, K.R. Seddon, Recalling COIL, *Green Chem*. 8 (2006) 411-414
2. M. Grätzel, *J. Photochem. Photobiol*. C *4* (2003) 145-153
3. I. Minami, *Molecules* 14 (2009) 2286-2305
4. B. Weyershausen, K. Lehmann, *Green Chem*. *7* (2005) 15-19
5. M. Matzke, S. Stolte, K. Thiele, T. Juffernholz, J. Arning, J. Ranke, U. Welz-Biermann, B. Jastorff, *Green Chem*. 9 (2007) 1198-1207
6. J. Ranke, A. Müller, U. Bottin-Weber, F. Stock, S. Stolte, J. Arning, R. Störmann, B. Jastorff, *Ecotoxicol. Environ. Saf*. 67 (2007) 430-438
7. S. Stolte, M. Matzke, J. Arning, A. Böschen, W.R. Pitner, U. Welz-Biermann, B. Jastorff, J. Ranke, *Green Chem*. 9 (2007) 1170-1179
8. S. Stolte, S. Abdulkarim, J. Arning, A.-K. Blomeyer-Nienstedt, U. Bottin-Weber, M. Matzke, J. Ranke, B. Jastorff, J. Thöming, *Green Chem*. 10 (2008) 214–224
9. J. Pernak, , I. Goc, , I. Mirska,**,** *Green Chem*. 6 (2004) 323-329
10. A. Latała, M. Nędzi, P. Stepnowski, *Green Chem*. 11 (2009) 580-588
11. T. P. T. Pham, C.-W. Cho, Y.-S. Yun, *Appl. Chem*. 11 (2007) 105-108
12. C. Comninellis and A. Nerini, *J. Appl. Electrochem*. 25 (1995) 23-28
13. M. Klavarioti, D. Mantzavinos, D. Kassinos, *Environ. Int*. 35 (2009) 402-417
14. P. Canizares, R. Paz, C. Saez, M.A. Rodrigo, *Electrochim. Acta* 53 (2008) 2144-2153
15. B. Louhichi, M.F. Ahmadi, N. Bensalah, A. Gadri, M.A. Rodrigo, *J. Hazard. Mater.* 158 (2008) 430-437
16. A. Ventura, G. Jacquet, A. Bermond, V. Camel, *Water Res*. 36 (2002) 3517-3522
17. R. Tolba, M. Tian, J. Wen, Z.-H. Jiang, A. Chen, *J. Electroanal. Chem.* 649 (2010) 9–15
18. J. Wua, H. Zhang, N. Oturan , Y. Wang, L. Chen, M. A. Oturan, *Chemosphere* 87 (2012) 614–620
19. P. Stepnowski, A. Zaleska, *Photochem. Photobiol*. 170 (2005) 45-50
20. E.M. Siedlecka, M. Gołębiowski, Z. Kaczyński, J. Czupryniak, T. Ossowski, P. Stepnowski, *Appl. Cat. B: Environmental* 91 (2009) 573-579
21. E.M. Siedlecka, W. Mrozik, Z. Kaczyński, P. Stepnowski, *J. Hazard. Mater*. 154 (2008) 893-900
22. A. Fabiańska, T. Ossowski, P. Stepnowski, S. Stolte, J. Thöming, E.M. Siedlecka, *Chem. Eng. J.* 198–199 (2012) 338–345C.
23. C. A. Martínez-Huitle, E. Brillas, *Appl. Cat. B,* 87 (2009) 105–145.

24. Comninellis, *Electrochim. Acta* 39 (1994) 1857-1862
25. E. Chatzisymeon, A. Dimou, D. Mantzavinos, A. Katsaounis, *J. Hazard. Mater*. 167 (2009) 268-274
26. L. Szpyrkowicz, M. Radaellis, S. Daniele, *Catalysis Today* 100 (2005) 425-429
27. M. Panizza, G. Cerisola, *Electrochim. Acta* 51 (2005) 191-199
28. F. Montilla, P. A. Michaud, E. Morallón, J. L. Vázquez, C. Comninellis *Electrochim. Acta* (2002) 3509-3513
29. J. Iniesta, P. A. Michaud, M. Panizza, G. Cerisola, A. Aldaz, C. Comninellis, *Electrochim. Acta* (2001) 3573-3578
30. I. Sires, E. Brillas, G. Cerisola, M. Panizza, *J. Electroanalyt. Chem*. 613 (2008) 151-159
31. M. Czerwicka, S. Stolte, A. Muller, E.M**.** Siedlecka**,** M. Gołębiowski, J. Kumirska, P. Stepnowski, *J. Hazard. Mater*. 171 (2009**)** 478-483I.